



UNIVERSITY OF LEEDS

This is a repository copy of *Comparison of the explosion characteristics and flame speeds of pulverised coals and biomass in the ISO standard 1 m³ dust explosion equipment*.

White Rose Research Online URL for this paper:
<http://eprints.whiterose.ac.uk/97723/>

Version: Accepted Version

Article:

Huescar Medina, C, MacCoitir, B, Sattar, H et al. (4 more authors) (2015) Comparison of the explosion characteristics and flame speeds of pulverised coals and biomass in the ISO standard 1 m³ dust explosion equipment. *Fuel*, 151. pp. 91-101. ISSN 0016-2361

<https://doi.org/10.1016/j.fuel.2015.01.009>

© 2015, Elsevier. Licensed under the Creative Commons Attribution-NonCommercial-NoDerivatives 4.0 International
<http://creativecommons.org/licenses/by-nc-nd/4.0/>

Reuse

Unless indicated otherwise, fulltext items are protected by copyright with all rights reserved. The copyright exception in section 29 of the Copyright, Designs and Patents Act 1988 allows the making of a single copy solely for the purpose of non-commercial research or private study within the limits of fair dealing. The publisher or other rights-holder may allow further reproduction and re-use of this version - refer to the White Rose Research Online record for this item. Where records identify the publisher as the copyright holder, users can verify any specific terms of use on the publisher's website.

Takedown

If you consider content in White Rose Research Online to be in breach of UK law, please notify us by emailing eprints@whiterose.ac.uk including the URL of the record and the reason for the withdrawal request.



eprints@whiterose.ac.uk
<https://eprints.whiterose.ac.uk/>

TITLE: Comparison of the explosion characteristics and flame speeds of pulverised coals and biomass in the ISO standard 1 m³ dust explosion equipment

AUTHORS: Huescar Medina (2 surnames), Clara*; MacCoitir, Brian; Sattar, Hamed; Slatter, D., Phylaktou, Herodotos N.; Andrews, Gordon E.; Gibbs, Bernard M.

AFFILIATION: Energy Research Institute, School of Chemical and Process Engineering, University of Leeds, Leeds, LS9 2JT, United Kingdom

***CORRESPONDING AUTHOR:**

Tel. +44 (0)113 3432493

Email: pm09chm@leeds.ac.uk or profgeandrews@hotmail.com

Address: Energy Research Institute, School of Chemical and Process Engineering University of Leeds, Leeds, LS9 2JT, United Kingdom

Abstract

Pulverised coal has been known to pose explosion risks since the 19th century, with the advent of biomass use in coal fired power generation boilers the explosion risk may need revision. The objective of the present work was to compare the explosibility of two samples of bituminous coal used in UK power stations with two biomass fuels and to review available explosion data in the literature for pulverised coal and biomass. The 1 m³ ISO explosion vessel was used to determine the explosion characteristics: deflagration index (K_{St}), maximum explosion pressure (P_{max}) and minimum explosible concentration (MEC). Flame speeds were also measured and these are relevant to understanding the mechanism of turbulent flame propagation in power station burners, which is related to the problem of flame flashback or blow-off. Despite the similarities in composition of both coals, the explosion reactivity of Colombian coal was much higher, with a K_{St} value of 129 bar·m/s

compared to 78 bar·m/s for Kellingley coal. The main difference between the two fuels was the surface area of particles which was higher for Colombian coal. It was shown that the char burn out rate at 900 °C in air was higher for Colombian coal, due to the greater oxygen diffusion in the higher porosity of the char. Results for two biomass fuels are also presented with similar values for K_{St} and the literature review shows that both coal and biomass have very variable flame reactivities. There is no general trend that coal is less reactive than biomass, although this could be the case for specific coals and biomass.

KEYWORDS: coal, dust explosion, combustion, flame propagation, biomass

1. Introduction

Coal is the major fuel used for generating electricity worldwide, generating 41% of the world's electricity [1] in 2012. In the UK, despite the introduction of renewable fuels for Greenhouse Gas (GHG) emission reduction, 29% of the electricity generated [2] is still produced from coal without carbon capture, in 40+ year old power plants. Pulverised coal combustion is the most commonly used method in coal-fired power plants [3]. It was back in the 19th century that coal dust clouds were first ignited by sparks. Since then extensive research efforts have been devoted to understanding coal dust explosibility and flame propagation [4]. Coal power plants present explosion risks in milling processes, transport of fuel to the boiler and during operation, start up and shut down of the boiler [5]. As a result these plants must comply with “Appareils destinés à être utilisés en **AT**mosphères **EX**plosibles” (ATEX); and Dangerous Substances and Explosive Atmospheres Regulations 2002 (DSEAR) to prevent or limit the effects of explosions. With the advent of biomass use in existing coal fired power stations, as a means of reducing fossil fuel CO₂ emissions, new explosion risks need evaluating including those due to dust generated in the enclosed biomass storage areas and the feed system to the stores and subsequent transport to the mills. This paper compares the coal and biomass explosion reactivities by measuring the K_{St} (Eq. 1) and turbulent flame speeds at constant pressure. These are compared with two biomass explosion characteristics and with literature values of coal and biomass reactivities.

$$K_{St} = \left(\frac{dP}{dt} \right)_{max} \cdot V^{1/3} \quad (1)$$

The design of safety systems such as venting or suppression requires the knowledge of the explosion characteristics of any hazardous dust, which include: the deflagration index (K_{St}) and the maximum explosion pressure (P_{max}), together with the concentration at which these occur. The minimum explosion concentration (MEC), limiting oxygen concentration (LOC), minimum ignition energy (MIE) and surface ignition temperatures are also required to be known. The methods for determination of explosion characteristics are outlined in the standard EN BS 14034. For the determination of K_{St} , P_{max} and MEC, which are considered in this study, explosion tests were performed in a 1 m³ explosion vessel within the flammable range. Pressure-time histories were recorded, the deflagration index (K_{St}) was derived according to Eq. 1 and the concentrations at which the maximum values of K_{St} and P_{max} occurred were determined.

Carbonaceous dusts explosibility was originally investigated using the Hartmann tube [5, 6], which is still used for MIE determinations and is allowed to be used for MEC measurements as it gives similar results to spherical explosion vessel methods. Current measurements of explosion peak pressure and deflagration index use spherical vessels with central ignition of a turbulent dust air mixture, as this is closer to adiabatic conditions, whereas the tube method suffers from flame contact with the vessel walls which reduces the peak pressure and the rate of pressure rise [5, 6]. Although the ISO 1 m³ spherical vessel is the reference standard for K_{St} and P_{max} measurements, the 20 L sphere is also recognised in the standards as it can be calibrated to give the same result. The 20 L sphere is in more common use than the 1 m³ due to the use of 1/50 of the mass of the dust to be tested and the lower cost of the equipment. The range of results in the literature for K_{St} and P_{max} for coal is shown in Table 1 and for biomass in Table 2. Biomass data is scarce as the standard equipment dust injection systems cannot operate for fibrous biomass as the dust delivery tubes block. Alternative biomass delivery systems are required and these then have to be calibrated with a reference dust to show agreement with the standard injector designs. The ignition delay between the start of injection and ignition is the

variable in the calibration. Details of the calibration used for biomass dust explosion are often not specified in the open literature.

Table 1. Explosion characteristics of different coals in the literature

Coal sample	K_{St}	P_{max}	Nominal MEC (g/m^3)	Particle size (μm)	Vessel volume	Reference
Morwell coal	220	7.6	-	$D_{50}=22$	20 L	[7]
Brown coal	151	10.0	-	$D_{50}=32$	1 m ³	
Yallourn dark	91	6.7	-	$D_{50}=36$	20 L	
Prince mine coal	44	6.5	70	<125	20 L	[8]
Phalen mine coal	30	6.0	120	<125	20 L	
Lingan mine coal	44	7.0	90	<125	20 L	
Russian anthracite	68	5.0	-	53	20 L	[9]
Sulcis lignite	162	6.8	-	53	20 L	
South African coal	81	6.0	-	53	20 L	
Polish coal	135	6.8	-	53	20 L	
Snibston coal	149	6.5	-	53	20 L	
Spanish lignite	107	8.8	90	$D_{50}=40$	1 m ³	[10]
German lignite	105	8.7	60	$D_{50}=58$	1 m ³	
Pittsburgh coal	41	6.7	65	<75	20 L	[11]
Pocahontas coal	31	6.5	80	<75	20 L	
Sebuku coal	114	6.6	63	$D_{50}=15$	20 L	[12]
Kellingley coal	80	8.2	120	$D_{90}=85$	1 m ³	Present work
Colombian coal	129	8.5	75	$D_{90}=65$	1 m ³	

Table 1 shows that for a diverse range of coal samples containing fine particles, mainly <75 μm , the explosion characteristics of coals can vary widely. K_{St} values range from 30 bar·m/s to 220 bar·m/s, P_{max} from 5 bar to 10 bar and MECs from 60 g/m^3 to 120 g/m^3 . This variability is due to the diverse composition and physical characterisation of the different coals. Table 1 shows that even though all the coals were milled to a small size, there were differences in the mean size and some correlation of this with K_{St} . For example Morwell coal with 22 μm mean size has the highest K_{St} of 220, but Sebuku coal with 15 μm size only has a K_{St} of 114 bar·m/s. The largest particle size results were <125 μm and the three coals of this size had the lowest K_{St} in Table 1 in the range 30-44. Comparison of coal reactivity as a function of coal composition has to be done at the same mean size and no such data has been published, as can be seen in Table 1.

A feature of the results in Table 1 that is difficult to explain is the variation of the peak pressure P_{max} . In spherical flame propagation the ratio P_{max}/P_i is the ratio of the peak flame temperature to initial temperature, assuming that the product to reactant mole ratio is close to 1. For gas flames the reactivity in the form of a burning velocity is directly related to flame temperature.

Table 2. Explosion characteristics of different biomass in the literature

Fuel	K_{St} (bar·m/s)	P_{max} (bara)	MEC (g/m ³)	Particle size (μ m)	Method	Ref.
Cork	179	7.2	40	$D_{90}=280$	20 L	[13]
Walnut shells dust	105	9.4	70	$D_{90}=311$	1 m ³	[14]
Pine nut shells dust	61	8.9	-	$D_{90}=439$		
Pistachio shells dust	82	9.3	90	$D_{90}=240$		
Wood	87	8.8	30	$D_{90}=700$	1 m ³	[10]
Bark	98	9.7	30	$D_{90}=700$		
Forest residue	84	9.1	60	$D_{90}=500$		
Spanish pine	23	8.2	90	$D_{90}=500$		
Barley straw	58	9.3	90	$D_{90}=500$		
Miscanthus	31	8.1	120	$D_{90}=350$		
Sorghum	28	8.2	120	$D_{90}=650$		
Rape seed straw	32	8.2	210	$D_{90}=500$		
Wood dust (beech and oak mix)	136	7.7	-	$D_{90}=125$	20 L	[15]
Forest residue (bark and wood)	92	9.1	20	$D_{50}=275$	20 L	[16]
Wood dust	87	7.8	-	-	20 L	[17]
Wood dust, chipboard	102	8.7	60	$D_{90}=43$	20 L/1 m ³	[4]
Wheat grain dust	112	9.3	60	<500		
Olive pellets	74	10.4	125	-		
Cellulose	66	9.3	60	125		
British Columbia wood pellets	146	8.1	70	<63	ASTM E1226	[18]
Nova Scotia wood pellets	162	8.4	70	<63		
Southern yellow pine wood pellets (USA)	98	7.7	25	<63		
Wood dust	208	9.4	-	-	1 m ³	[19]
Fibrous wood	149	8.2	20	<75	20 L	[20]
Sawdust	115	9.0	-	-	1 m ³	[21]
Dry Douglas Fir & Western Red Cedar	43	8.5	-	250	20L	[22]
Dry Mountain Pine & Lodgepole Pine	40	8.8	-	200	20L	
Dry Spruce & Pine & Fir	51	8.2	-	$D_{90}=200$	20L	
Southern Pine	105	9.0	-	$D_{90}=739$	1 m ³	Present work
Norway Spruce	95	9.2	-	$D_{90}=603$	1 m ³	

Coal dusts data in Table 1 do not show this relationship and the highest K_{St} coal has a rather modest P_{max} of 7.6 bar. However, all the highest P_{max} in Table 1 are for explosions in the ISO 1 m³ vessel and

all the low P_{\max} are for the 20L sphere. These vessels appear to be too small to achieve complete combustion and no contact of the flame with the wall until all the coal has been burned. In the authors experience the 10 kJ igniters in the 20L sphere and 1 m³ give a line ignition source and not a central ignition. In the 20 L sphere the ignitor jet impinges on the wall and the combustion proceeds in contact with the wall which reduces the peak pressure. This effect is reduced in the 1 m³, but is avoided in the present work by making the ignitor jet impinge on a hemispherical grid which results in a central ball of hot ignition gas. The flame speed records in three directions show that spherical flame propagation was achieved.

The present results for experiments in the ISO 1 m³ vessel, as detailed later, are summarised in Table 1 for the two coals studied. The present results show higher P_{\max} than for all the 20 L results in the literature and in good agreement with the other 1 m³ results in Table 1. The K_{St} results are within the data spread for other coals in Table 1. There are less reactive coals than Kellingley and there are more reactive coals than the present Colombian coal, but they are representative of low and high reactivity coals in the literature. These two coals with significantly different K_{St} , are shown below to have a very similar composition. The reason for the reactivity difference will be shown to be physical coal structure differences and not chemical differences.

Table 2 shows that the literature data for biomass explosions shows a wide range of K_{St} and a high sensitivity to particle size. Comparison with Table 1 shows that peak pressures are often higher with biomass, indicating higher flame temperatures in spite of the lower calorific values. This is likely to be due to the lower ash content of biomass compared with coal. The ash acts as a heat sink that cools the flame. The MEC are also significantly leaner for biomass fuels compared with coal and this indicates a higher reactivity. However, the range of K_{St} is similar to coal and it cannot be concluded that biomass is more reactive than coal, although there are individual biomass that are more reactive than some coals. Most of the biomass samples contain larger particles than coal as biomass is more difficult to mill to the size coal can be milled. The presence of larger particles for biomass reduces their reactivity and K_{St} , but does not reduce the peak temperature of the flame and hence the pressure

rise. The variability of K_{St} in Table 2 is partially due to size variability and partially due to composition differences, but most of the references do not have a detailed fuel analysis. In the present work the two biomass fuels are analysed in detail and the results summarised in Table 2 show that the present biomass fuels are typical of the range of biomass in the literature, with some biomass having higher K_{St} and others having much lower K_{St} , often because of the large particle sizes used.

Coal dust flame propagation mechanisms have been the object of research for many years. It is generally accepted that the combustion process of coal particles consists of devolatilisation and subsequent reaction of volatile components, heterogeneous char surface reactions as well as other physiochemical changes to the particles [23]. These processes are not only affected by the coal type, dust concentration and particle size distribution but by the heating rate, final temperature, residence time and quench process [24]. The heating rate in turbulent propagating pulverised coal flames is high in dust explosion equipment and in boiler flames. The flame temperature in spherical vessel explosions with central ignition is close to the adiabatic temperature as the only heat losses from the flame are radiation to the wall or dust ahead of the flame and heat loss to the ignitor which is low [25]. For a turbulent coal dust cloud propagating at between 1 m/s and 5 m/s, which the present work will show is a realistic range, the residence time in a 10 mm thick preheat zone and a 2000 K flame temperature is between 0.2 and 1×10^6 K/s. Laboratory techniques for studying coal or biomass particle oxidation, such as TGA or drop tube reactors have heating rates orders of magnitude below those in practical turbulent flame propagation. Typically TGA heating rates are 0.2 – 1 K/s, a factor of 10^6 below reality and drop tube furnaces heating rates are typically of order 5000 K/s which are a factor of between 40 and 200 below real flame heating rates. It is known that high heating rates increase the yield of volatiles from coal and biomass [26] and hence the ability in the present work to investigate pulverised coal and biomass at practical heating rates is crucial to the production of useful flame heat release data.

Hertzberg et al. [27] suggested that the char oxidation rate is too slow to make a significant contribution to flame propagation and therefore considered that char acted as a heat sink. The present

work will show that this cannot explain the fast propagation of coal and biomass flames, as the peak pressure rise is close to equilibrium, indicating that there has been little heat loss that would reduce the peak temperature.

This approach has been considered for the modelling of coal dust explosions more recently [25, 28], but fails to take into account known MEC data for coal and other HCO dusts (i.e. organic dusts). The MEC data shows that the equivalence ratio for the MEC of many HCO dusts is leaner than that for a gaseous hydrocarbon [29]. As a model that presumes the volatiles are hydrocarbons and the flame is a hydrocarbon flame, this cannot explain why a dust that has volatiles <100% of the mass can have a lean limit leaner than 100% hydrocarbon gas. Other researchers pointed out that the Hertzberg et al. [27] model fails to consider the possible effects of particle structure on explosibility [7, 30].

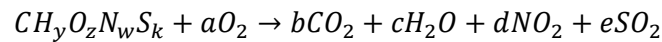
Woskoboenko [7] suggested that for certain coals surface area could greatly affect the explosion reactivity as the rates of devolatilisation and char burnout are faster and the present results support this conclusion.

The objectives of the present work were to measure the explosion characteristics (MEC, K_{St} , P_{max}) of pulverised Colombian coal and Kellingley coal and compare with two pulverised biomass explosions. The laminar and turbulent flame speeds and burning velocities were determined. This is the essential data required in burner design to avoid flame flashback and blow-off. In addition residues collected after explosion tests were analysed in order to understand why roughly half of the coal or biomass injected did not participate in the flame propagation. This unburned coal or biomass was not in the flame zone and did not act as a heat sink; otherwise the adiabatic pressure rise could not be achieved. The work also examines the reason that coal and biomass reactivity are so variable, even when the chemical composition is similar.

2. Experimental methods

2.1. Fuels and their characterisation

Samples of Colombian and Kellingley coal were supplied in pulverised form by Moneypoint (Ireland) and Drax (England) power stations respectively. The original fuels and some samples of residue collected after the explosion tests were analysed for their composition through elemental and TGA-proximate analysis using a Flash 2000 Thermoscientific C/H/N/S analyser (oxygen content was calculated by subtraction), and a TGA-50 Shimadzu analyser respectively. The elemental composition was used to derive the stoichiometric fuel to air ratio. Assuming the fuel formula is $CH_yO_zN_wS_k$ where y , z , w and k are the atomic ratios to carbon of hydrogen, oxygen, nitrogen, and sulphur respectively, and assuming the combustion reaction was:



The stoichiometric fuel to air mass ratio is given by:

$$\text{Stoichiometric } (F/A) = \frac{(12 + y + 16z + 14w + 32k)}{137.3 \left[\left(1 + \frac{y}{4}\right) - \frac{z}{2} + w + k \right]} \quad (2)$$

The stoichiometric (F/A) ratio can be expressed as grams of fuel per cubic meter of air by multiplying the stoichiometric fuel to air mass ratio by the density of air (1200 g/m^3). In addition, the concentration of dust clouds was expressed as an equivalence ratio (ratio of actual to stoichiometric concentrations). The gross calorific value (GCV) of all samples was determined in a Parr 6200 bomb calorimeter to the specifications of BS ISO 1928:2009 [31]. Bulk densities of all pulverized fuels were determined weighing increasing amounts of fuels in a known volume. The results were expressed as the average of 10 measurements. Furthermore, the density of particles (true density) was measured using an AccuPyc 1330 Pycnometer.

The morphology of particles before and after explosion was assessed through Scanning Electron Microscopy (SEM) images using a Carl Zeiss EVO MA15 instrument and the particle size distributions were determined using a Malvern Mastersizer 2000 instrument. The surface area and

porosity of fuels were also determined through Brunauer–Emmett–Teller (BET) analysis in a Micrometrics Tristar 3000 analyser.

2.3. Explosion characterisation: ISO 1 m³ vessel

Explosion tests were performed using the ISO 1 m³ vessel according to the methods recommended by the European standard EN BS 14034. The set-up consisted of a 1 m³ volume explosion chamber connected through a 19 mm internal diameter pipe to an external 5 L dust holder (Fig.1).



Figure 1: Leeds ISO 1 m³ vessel

Initially the dust sample was loaded into the external dust holder and pressurised to 20 bar. A fast acting valve separated both the dust holder and explosion chamber. On activation of the valve the dust was pushed through the delivery system and dispersed inside the explosion chamber through the standard multi-hole C-tube. After an ignition delay of 0.6 s from the start of dust dispersion into the vessel, ignition of the dust took place by means of two 5 kJ chemical igniters placed in the geometric centre of the explosion chamber, firing into a perforated hemispherical cup to ensure central ignition and spherical propagation. Prior to dispersion of the dust from the dust holder, the explosion chamber

was evacuated so that on addition of the dust from the dust holder, the initial pressure at the time of ignition was 1.013 bar.

It was found that the standard 'C' ring dust disperser did not allow fibrous biomass milled to $<63\mu\text{m}$ to pass and compressed it as a pellet in the 'C' ring. The only type of biomass that would pass through the conventional injection system was nut shells and the results for walnut, pine nut and pistachio nut shell dusts milled and sieved to $<63\mu\text{m}$ were presented by Sattar et al. [14] for a nominal dust concentration of 750 g/m^3 . For fibrous biomass milled and sieved to $<63\mu\text{m}$ a new injector was developed and calibrated with a 10 L external dust container for low bulk density biomass [32] and a spherical nozzle dust disperser as shown in Fig. 2. This was calibrated for its ignition delay using cornflour to give the same K_{St} with the standard 'C' ring disperser and the 10 L external dust store and spherical nozzle disperser.



Figure 2. New spherical nozzle disperser for fibrous biomass $<63\mu\text{m}$

After an explosion in the 1 m^3 vessel, dust residues were found both in the dust holder (not injected) and in the explosion chamber [29, 33]. The dust found in the dust holder did not participate in the combustion reaction and therefore it was accounted for to correct the amount of dust present inside the explosion chamber (injected concentration). However, the dust that remained in the explosion chamber was a mixture of burnt, partially burnt and unburnt material. All residues were collected and

weighed using a vacuum cleaner with the filter bag new for each sample and weighed before and after collecting the dust. Only the residue found for the most reactive concentration was analysed in order to understand its role during the explosion test. The mass of the residue was deducted from the mass injected to give the mass burned and this was converted into a burned gas flame front equivalence ratio. The authors [33] have shown for biomass that the mechanism for the unburned fuel is that the explosion induced wind ahead of the flame entrains particles and carries them to the wall without them participating in the flame front flame propagation. On the wall they form a thin compressed layer that insulates the flame from the vessel wall and thus reduces the heat loss and the pressure decay. The layer of the deposit that the flame impinges on undergoes some pyrolysis. In this work it is shown that the same mechanism applies in coal dust explosions.

The vessel was fitted with Keller PA11 piezoresistive pressure transducers for recording of pressure-time histories and also with arrays of exposed junction type-K thermocouples in the horizontal (left and right) and vertical (downwards) directions.

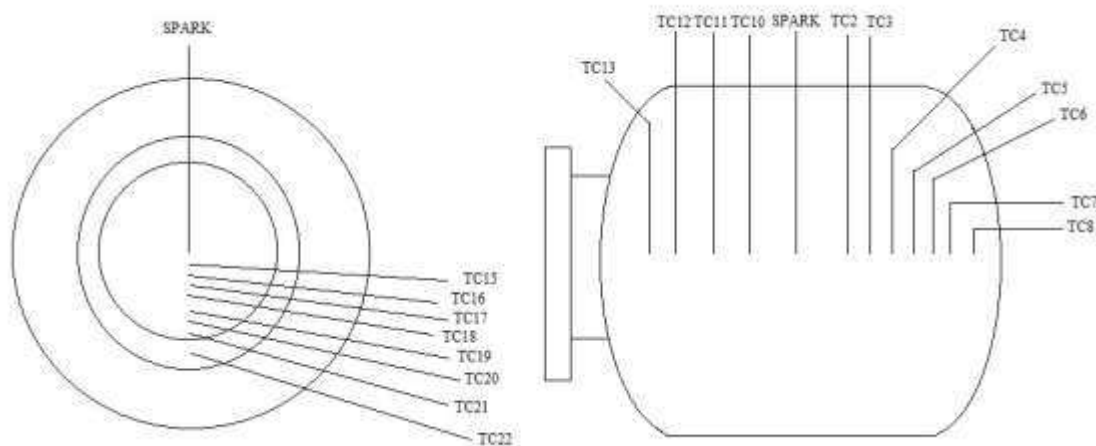


Figure 3. Thermocouple arrangement in the 1m³ vessel

These thermocouples allowed determination of times of flame arrival to each thermocouple position and derivation of flame speeds in all directions [34]. The overall radial turbulent flame speed $(S_F)_T$ for a given test was the average of the flame speed in each direction. The maximum pressure and the

maximum rate of pressure rise for a given mixture were derived from the pressure-time records. The maximum pressure (bara) for a given mixture of dust was normalised to the initial pressure (bara) at the time of ignition (P_i).

Turbulent flame speeds can be used for the design of safety systems and for modelling of explosions but also for burner design. Turbulent $(S_F)_T$ and laminar (S_F) flame speeds are related as follows [35],

$$(S_F)_T = \beta \cdot S_F \quad (3)$$

where β is the turbulence factor of the vessel. β is a parameter used in venting correlations to account for the turbulence created by obstacles in the path of the flame. Here is used to account for the turbulence induced due to the dispersion of dust. β was found to be 4.03 for the Leeds 1 m³ ISO vessel by performing laminar and turbulent gas explosions. Adding pressurised air from the dust pot provided an analogous turbulence to that present in dust explosions [34]. Eq. 3 was used to determine the laminar flame speed and by dividing this by the adiabatic expansion ratio the laminar burning velocity could be determined [34].

The MW per unit area of the flame front (heat release rate or HRR) was calculated using the following expression:

$$HRR \left(MW/m^2 \right) = \frac{(S_F)_T}{\left(\frac{P_{max}}{P_i} \right)} \rho_u \frac{GCV}{(1 + A/F)}$$

Where ρ_u was taken as the unburnt air density 1.2 kg/m³ and A/F was the corresponding flame front air to fuel ratio (i.e. “as fired” or “as received” A/F ratios).

3. Results and discussion

3.1. Fuel characterisation

Characteristics of the two coal fuels and two biomass fuels used for comparison are shown in Table 3. The main difference between both bituminous coal samples was found in the particles surface area. The surface area of Colombian coal particles was 4.3 times higher than that of Kellingley coal. The pore volume for Colombian coal was also more than two times higher than that of Kellingley coal. Table 3 shows that the difference in fuel properties and composition between the two coals was relatively small compared with the large difference in surface area. The biomass composition showed the well known much higher volatile content compared with coal and much lower ash content. The stoichiometric air to fuel (A/F) ratios are significantly lower for the biomass fuels as are the calorific values. It is significant that the biomass particle surface areas are well below those for coal and also have much lower pore volume. The different reactivities of the two coal samples in Table 1, with little difference in fuel properties, are thought to be due to the large difference in surface areas. However, both biomass fuels are more reactive than Kellingley coal and yet have a lower surface area. This indicates a different mechanism of flame propagation for biomass than for coal.

Table 3. Fuel characterisation

	Kellingley coal	Colombian coal	Norway spruce	Southern pine
Bulk density (kgm^{-3})	443	407	176	268
True density (kgm^{-3})	1480	1450	1409	1491
Surface area (m^2g^{-1})	3.7	15.8	0.7	1.7
Pore volume mm^3g^{-1}	14	32	2.4	7.3
GCV (MJkg^{-1}) _{daf}	33.8	33.5	21.2	20.8
Elemental Composition (w/w, daf)				
C	82.1	81.8	53.4	52.4
H	5.2	5.3	6.2	5.8
N	3.0	2.5	0.0	0.7
S	2.8	0.9	0.0	0.0
O	7.0	9.5	40.4	41.2
Proximate analysis (w/w, as received)				
Moisture	1.7	3.2	5.8	5.0
VM	29.2	33.7	79.0	78.5
FC	50	47.8	11.1	14.0

Ash	19.1	15.3	4.1	2.5
Stoichiometric (A/F)	11.3	11.1	6.5	6.3
Stoichiometric F/A (gm ⁻³)	106	108	184	190

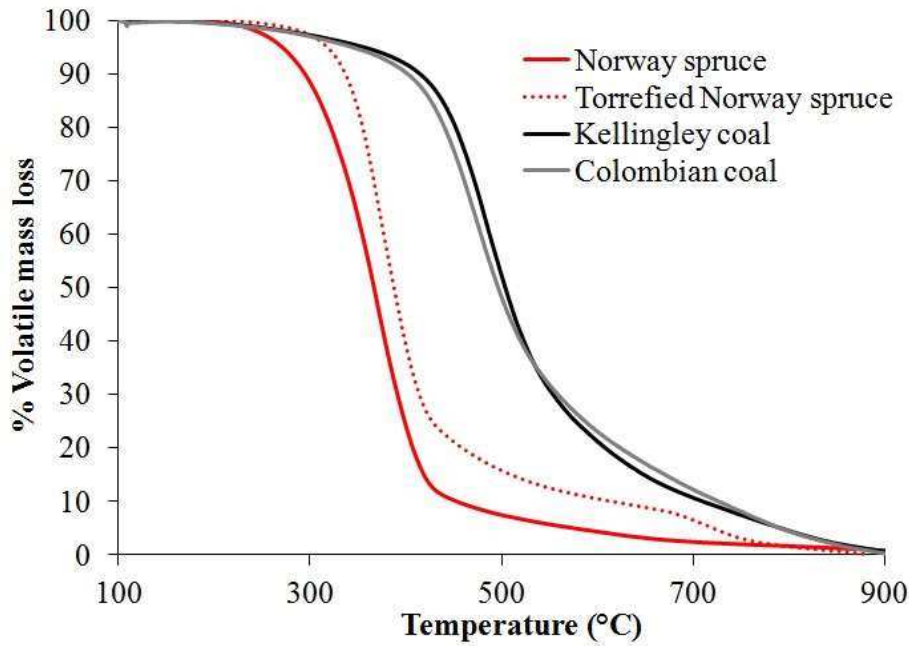


Figure 4. Volatiles mass loss of Kellingley and Colombian coal

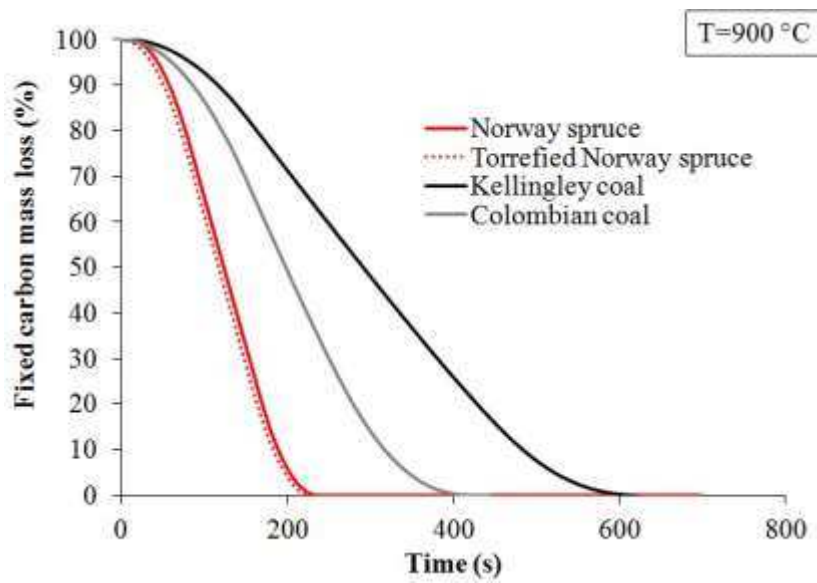


Figure 5. Fixed carbon oxidation rate in air at 900°C of Kellingley and Colombian coal

The TGA normalised volatile mass loss in a nitrogen atmosphere between 100 and 900 °C is shown as a function of temperature in Fig. 3. The nitrogen was changed to air at 900 °C and the normalised carbon mass is shown as a function of time in Fig.4. Both coals had very similar rates of volatile mass loss. However, the carbon oxidation mass loss rate was 1.8 times faster for Colombian coal. The higher surface area of Colombian coal clearly enhanced the rate at which the char was burnt and this is likely to be due to the greater access of oxygen into the char pores, which would be higher for Colombian coal due to the initial higher porosity of the coal.

Fig. 5 shows that the two coals had very similar size distribution and Table 4 shows that the various mean sizes were slightly smaller for Kellingley coal. Fig. 5 also shows the size distribution for two biomass fuels and this shows that they had a much wider size distribution. Table 4 shows that the mean sizes were also much higher than for coal.

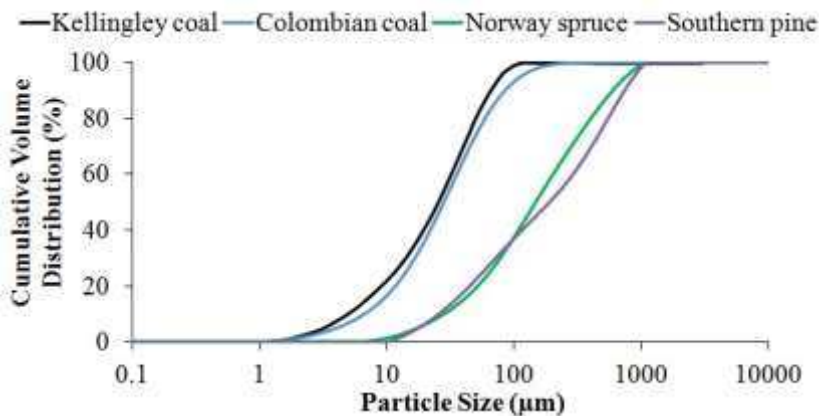


Figure 6. Cumulative volume distribution of Kellingley and Colombian coal, Norway spruce and Southern pine

Table 4. Particle size analysis parameters

	Surface weighted mean diameter D[3,2] (µm)	Volume weighted mean diameter D[4,3] (µm)	D ₁₀ (µm)	D ₅₀ (µm)	D ₉₀ (µm)
Kellingley Coal	12	31	5.0	25.5	65.3
Colombian coal	15	40	6.8	28.1	85.2
Norway spruce	71	239	28.4	148.5	602.7
Southern pine	72	294	25.4	189.8	739.4

SEM images were used to assess the morphology of coal particles of both samples. Coal particles typically present angular and sharp edges [36, 37]. Fig.6 present SEM images of Kellingley and Colombian coal were the characteristic features of coal particles were confirmed.

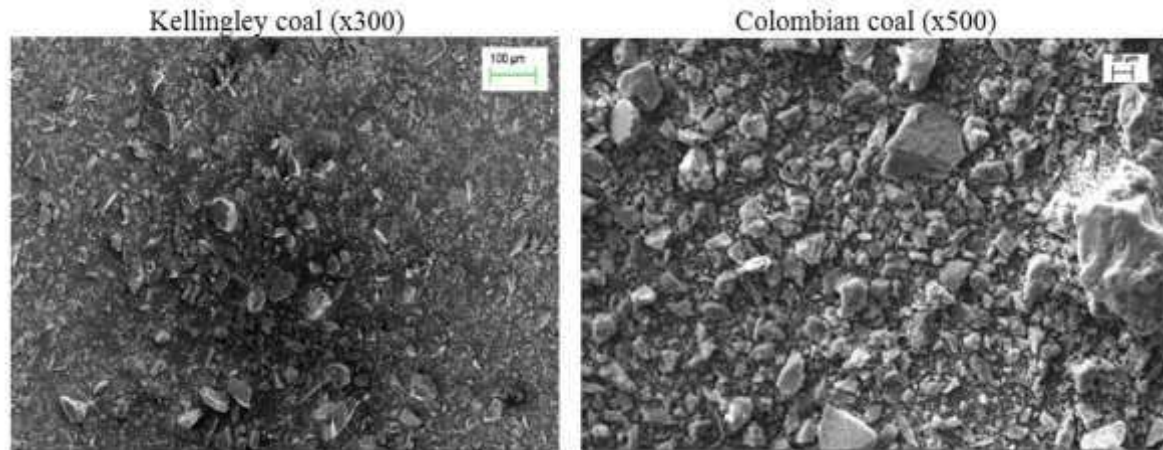


Figure 7. SEM images of Kellingley (left) and Colombian (right) coal

3.2. Explosion characterisation

K_{St} and pressure ratios are presented in Fig.7 as a function of the corrected (burnt) equivalence ratio. Colombian coal had a maximum K_{St} value 1.7 times higher than that of Kellingley coal, which is very close to the carbon oxidation ratio. This indicated a faster rate of combustion. The maximum explosion pressure for Colombian coal at 8.5 bar was only 4% higher than for Kellingley coal. In comparison to literature K_{St} values for other coal types, Colombian coal was comparable to the more reactive coals reported in Table 1 and Kellingley coal to the least.

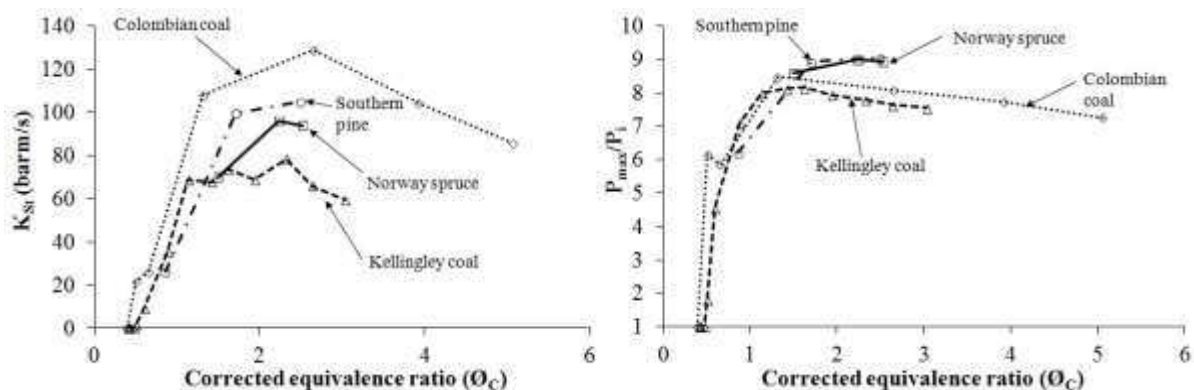


Figure 8. K_{St} and pressure ratio as a function of injected equivalence ratio

Despite the similarities in composition the reactivity of Colombian coal was found to be significantly higher than that of Kellingley coal. The maximum pressure is dependent on the energy content of the fuel/air mix and the heat losses. Since both samples had similar calorific values the difference in maximum pressure was not large. The greater difference in K_{St} indicates that the rate of mass burning was markedly different for each of the samples. The rate of mass burning in this case is most likely affected by surface area. It was pointed out in section 3.1 that the surface area of Colombian coal was distinctly higher than that of Kellingley coal. It is generally accepted that when heating rates are high the amount of volatiles released is increased in comparison to that detected under proximate analysis techniques. The increase of volatiles due to high heating rates should be similar for both samples. However, the rate of volatile release and combustion could be enhanced due to the higher surface area of Colombian coal. The rate of char burnout could also have been increased due to the greater surface area.

The minimum explosive concentration (corrected) for Colombian coal was 43 g/m^3 ($\phi=0.4$) and 50 g/m^3 ($\phi=0.5$) for Kellingley coal. Colombian coal was more reactive in its MEC as well as its K_{St} . These coal MECs are richer than those usually found for biomass dusts $<63 \mu\text{m}$ [38]. In the present work with biomass particle sizes $\gg 63 \mu\text{m}$ the MEC were richer than for finer particles and were similar to the coal particles at a burned mass equivalence ratio of 0.5. All these MEC equivalence ratios are close to that for pure hydrocarbon gases. This shows that coal and biomass MEC cannot be explained by the volatiles being hydrocarbons as this would require 100% of the particle mass to be hydrocarbons and this is impossible as there is insufficient hydrogen or volatiles in the coal and insufficient hydrogen in biomass.

Flame speeds were measured using the thermocouple arrays fitted to the 1 m^3 explosion vessel. An example of a flame position against time plot obtained for Colombian coal is shown in Fig.8. The position of the flame over time was mapped out in three directions: horizontal right and left and vertical downwards. The slope of a linear fit to the positions in each direction corresponded to the flame speed in each direction. The average flame speed for a single test is the average of the flame

speeds in each direction and is represented in Fig.8 by the average radial flame position line. All three lines in Fig. 8 are reasonably parallel and this shows that a spherical flame had been achieved. Similar results were found for biomass explosions.

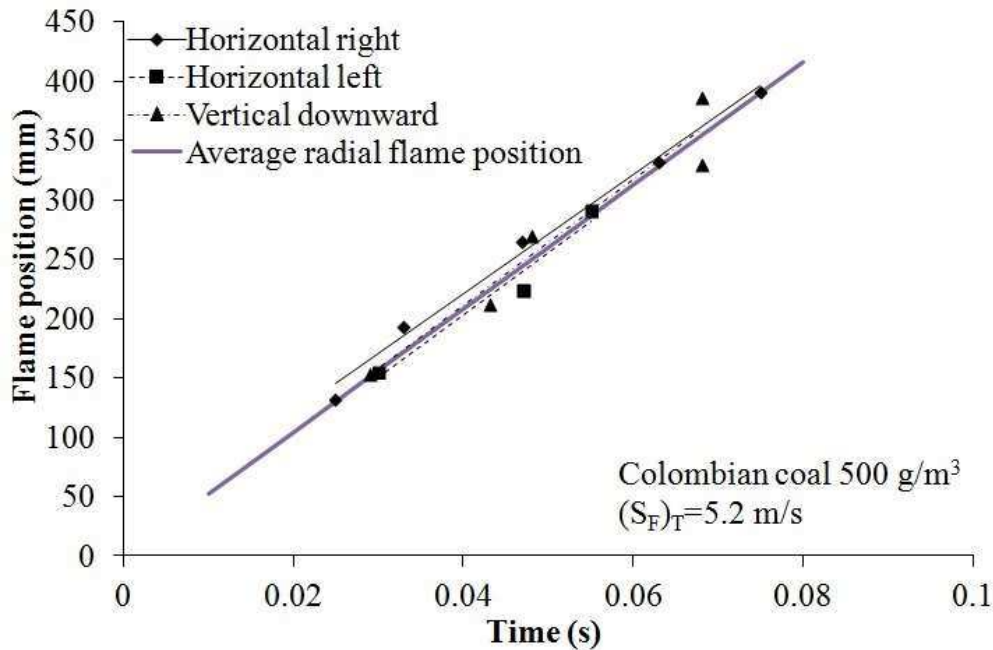


Figure 9. Example flame position graph and derivation of flame speeds

The maximum flame speed for Kellingley coal was 3.7 m/s, whereas it was 5.2 m/s for Colombian coal (the ratio of maximum flame speeds was 1.4, also close to the carbon burnout ratio of 1.8). Using the turbulence factor obtained for this explosion vessel (4.03) the corresponding laminar flame speeds were 0.9 m/s and 1.3 m/s. These values are comparable to values quoted in the literature for other coals [23]. If the ratio of the peak to initial pressures is used for the expansion ratio then the laminar burning velocities are 0.12 m/s and 0.16 m/s, which are considerably below the laminar burning velocity of hydrocarbons which are about 0.4 m/s.

The variation of flame speeds, burning velocities and global heat release rates with burnt equivalence ratio is shown in Fig.9. At typical coal burner operation (20% excess air) the global heat release rates were 3 MW/m² and 5 MW/m² for Kellingley coal and Colombian coal respectively. These values are comparable to coal burner measurements quoted in the literature [39, 40]. Therefore the combustion

data produced through the 1 m³ explosion vessel method is relevant to understanding the mechanism of turbulent flame propagation in power station burners, which is related to the problem of flame flash back of blow-off. Fig. 9 also shows that global heat release rates are lower for the biomass samples, mainly due to the lower calorific values, as the flame speeds are similar to Kellingley coal.

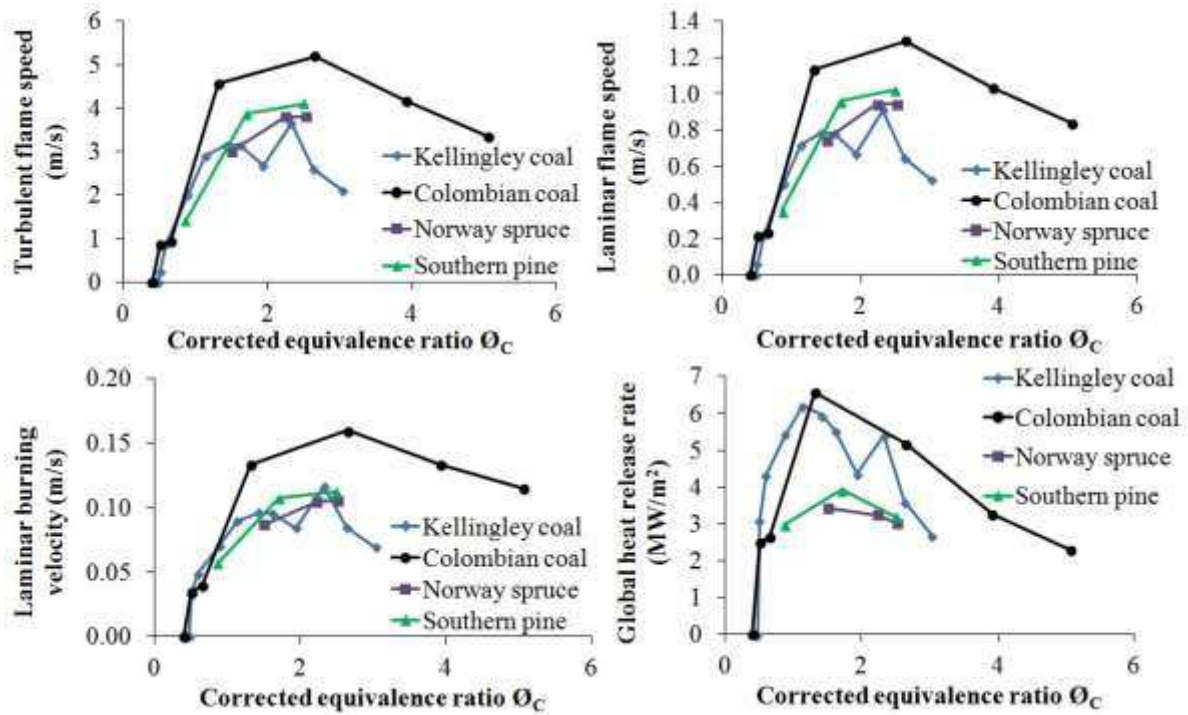


Figure 10. Turbulent and laminar flame speeds, burning velocity and heat release rates as a function of burnt equivalence ratio

The biomass fuels have a low surface area and porosity, as shown in Table 3, which is lower than but similar to Kellingley coal. The similarity of the biomass flame speeds and burning velocities with Kellingley coal was surprising as the biomass have very high volatiles and Kellingley coal has very low volatiles, as shown in Table 3. Kellingley coal also has much higher ash content than both of the biomass and this would normally act as a heat sink to lower flame temperatures and this would lower the burning velocity. The implication of these results is that it is not just the volatiles in the fuel that propagate the flame, the carbon or char must also burn to give the high temperatures that are responsible for the high peak pressures. This is not the conventional model of pulverised coal and

biomass flame, where volatile release and hydrocarbon combustion used in most CFD furnace models.

3.3. Analysis of residues

Residues collected after explosion tests of the most reactive concentrations were weighed and analysed following the same procedures as with the original samples and the results are summarised in Table 5. In explosion tests with coal it was not possible to distinguish visually whether particles were burnt or unburnt, but for biomass the debris after the explosion had black particles scattered in the original biomass that had not burned completely. In previous work carried out with woody biomass samples by the authors [33] it was found that the residues formed a layer on the wall of the vessel where the particles closest to the wall appeared unreacted and particles exposed to the impinging flame consisted of black particles due to pyrolysis by the quenching flame. The mechanism is that the explosion induced wind ahead of the expanding flames entrains some particles ahead of the flame and carries them to the wall region, so that they do not participate in the flame propagation. The pressure rise compresses the particles in the wall region and the flame impinges and quenches on the outer surface of the deposits [33].

Assuming that the layer of residue was homogeneously distributed in the vessel walls and considering the vessel spherical, a theoretical layer thickness was calculated. The predicted thickness of the layer increased as more dust was present in the vessel (see Fig.10). The rate of pressure loss could also be derived using the pressure-time histories. The rate of pressure loss was defined as:

$$\text{Rate of pressure loss} = \frac{P_{max} - 0.9P_{max}}{\Delta t} \quad (4)$$

Rates of pressure loss and layer thicknesses for Kellingley and Colombian coal are also shown in Fig.10. The rate of pressure loss increased for lean mixtures as the flame temperature increased. However, after the maximum flame temperatures were achieved for mixtures slightly richer than stoichiometric the pressure loss started decreasing. It is known from the maximum explosion pressure

plot (Fig. 7, right) that pressure remained fairly constant for rich mixtures which indicated that flame temperatures also remained constant.

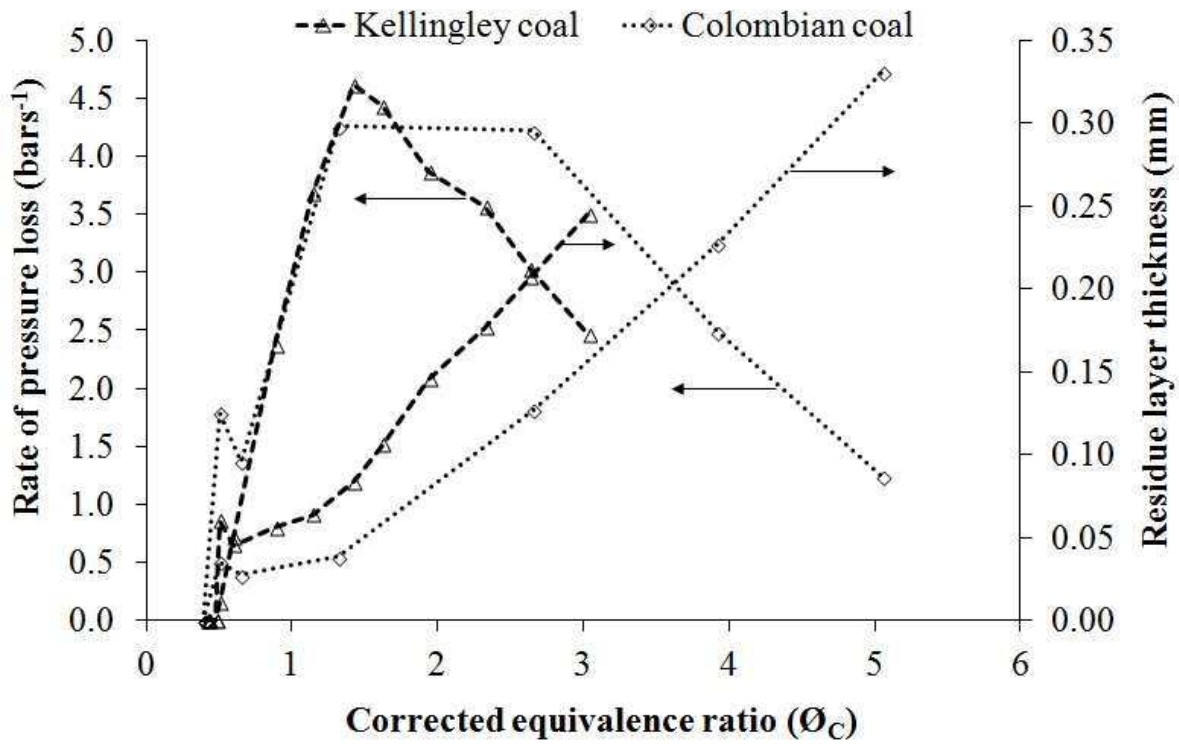


Figure 11. Rates of pressure loss and layer thickness as a function of corrected (burnt) equivalence ratio

Therefore, for rich mixtures the decrease in rate of pressure loss should have remained constant. However, because the thickness of the layer created was increased as more dust was injected the rate of pressure loss decreased. This phenomenon did not take place when methane gas explosions were performed in the same 1 m³ explosion vessel [33]. Figure 11 shows a comparison of the rate of pressure loss between gas propane and the two coal dusts used in this study. The rates of pressure loss with gases were much higher since no insulating layer was formed and heat was lost faster through the vessel walls.

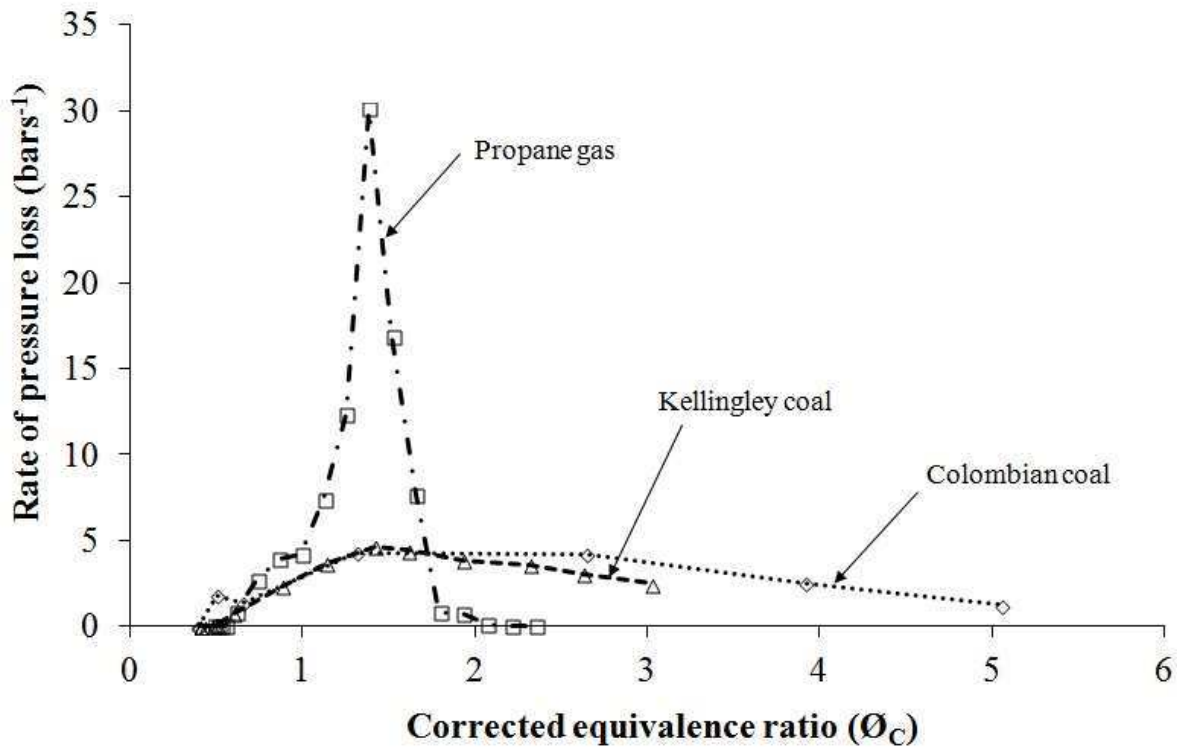


Figure 12. Comparison of rates of pressure loss of gas propane and coal dusts

Previous work by Slatter et al. [33] used a density separation method to isolate burned, partially burned and unreacted particles. However, in this study the residue samples were analysed as a bulk mass. Table 5 presents the elemental and proximate analysis of the original coal samples and residue samples. The percentage change with respect to the original sample is presented in brackets. The elemental composition of the residues was different from that of the original sample. The TGA analysis showed that volatiles were lost. The variations in elemental composition were therefore due to the loss of volatiles.

Another feature of the residues was that both the ash and fixed carbon increased. This is to be expected as the coal that burns in the flame front must leave the coal ash in the deposits. The results show that the increase in ash and carbon in the debris was smaller for Kellingley coal than for Colombian coal. This was due to Colombian coal being more reactive than Kellingley coal.

Kellingley coal ash in the deposits would ascend to 13% of the mass of residue. Overall, the mass of residue contained 19.9% of ash, therefore the remainder 7% of the ash contained in the residue was

formed as a result of pyrolysis in the wall. Similarly, Colombian coal ash deposits would account for 15.6% of the residual mass, the remainder 13% of ash resulted from pyrolysis at the wall. Therefore due to the action of the cooling flame front on the layer of Colombian coal at the wall, 41g of ash were formed compared to 29 g with Kellingley coal. The ratio, 1.4, is also close to the 1.8 ratio between char burnout rates of Colombian and Kellingley coal.

Table 5. Analysis of most reactive mixture explosion residue of Kellingley coal and Colombian coal

	Pre-Explosion	Post-Explosion
Fuel Sample	Kellingley coal	Kellingley coal (Change %)
Elemental analysis (% by mass) _{daf}		
C	65.0	64.3 (-1)
H	4.1	3.5 (-15)
O	5.5	7.1 (+29)
N	2.4	1.4 (-42)
S	2.2	2.2
TGA-Proximate (% by mass)		
Moisture	1.7	1.6 (-6)
Ash	19.1	19.9 (+4)
Volatile Matter	29.2	25.0 (-14)
Fixed Carbon	50.0	53.5 (+7)
Fuel Sample	Colombian coal	Colombian coal (Change %)
Elemental analysis (% by mass) _{daf}		
C	66.6	61.8 (-7)
H	4.3	2.1 (-51)
O	7.8	2.7 (-65)
N	2.1	1.7 (-19)
S	0.7	0.9 (+29)
TGA-Proximate (% by mass)		
Moisture	3.2	2.2 (-31)
Ash	15.3	28.5 (+86)
Volatile Matter	33.7	14.4 (-57)
Fixed Carbon	47.8	54.9 (+15)

Further proof of the proposed residue formation mechanism is given by the SEM images of the samples after explosion tests in Figure 12. SEM images of the residues (right images) show that original particles were mixed with bigger and structurally different char particles. This confirms that a layer of particles likely to be closest to the wall when the flame front impinged remained unchanged.

Char particles (closest to the flame front) became molten and formed large clusters of round surfaces with blow out holes, as has been previously reported in the literature [36, 37]. This resulted in residues having different size distribution compared to the original sample. Fig. 13 confirms that the deposits had larger particles than the original sample. It was shown that for biomass the presence of char particles in the residue was much less or almost inexistent and therefore the size distribution of the residues was very similar to the original samples [41]. It can therefore be ruled out that the difference in size distribution between original samples and deposits was due to preferential burning of fine particles or agglomeration due to compression of particles in the wall.

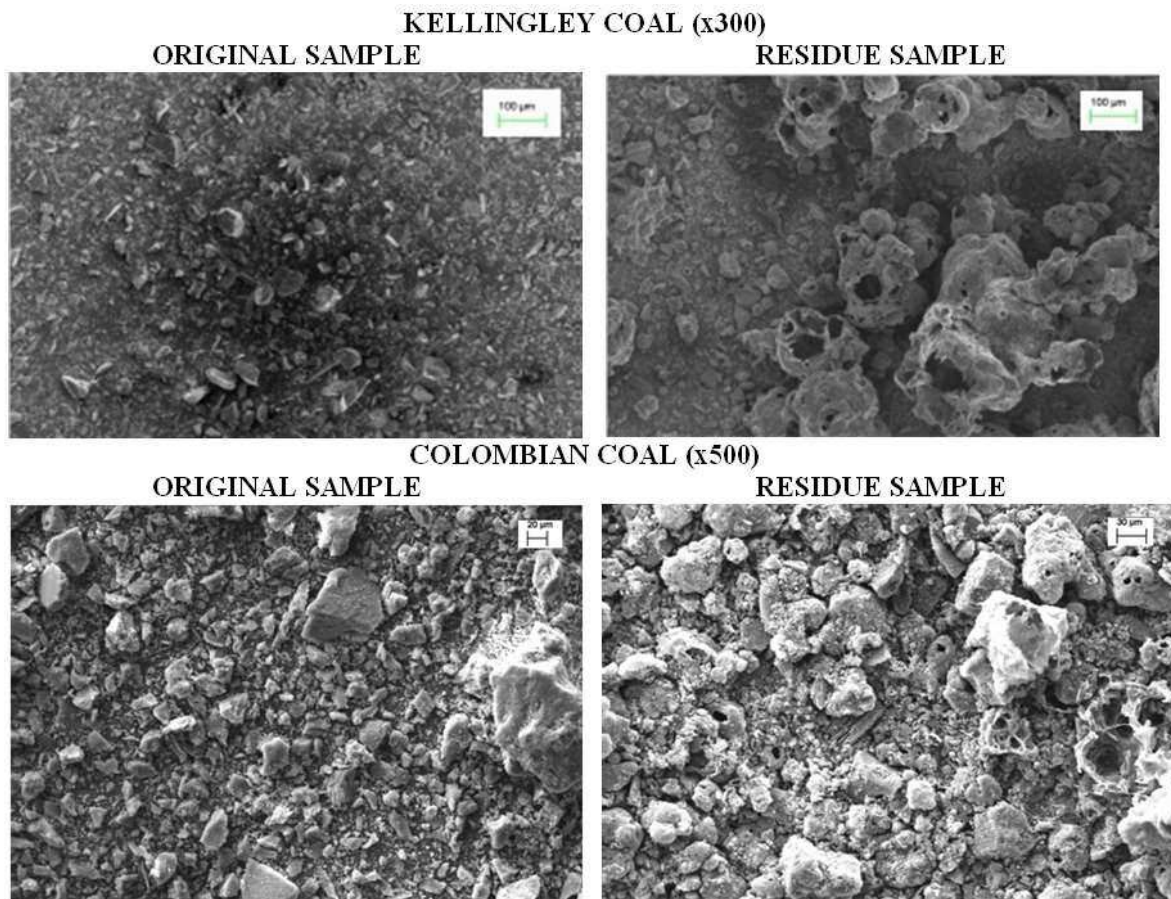


Figure 13. SEM images of original and residual samples of Kellingley coal and Colombian coal

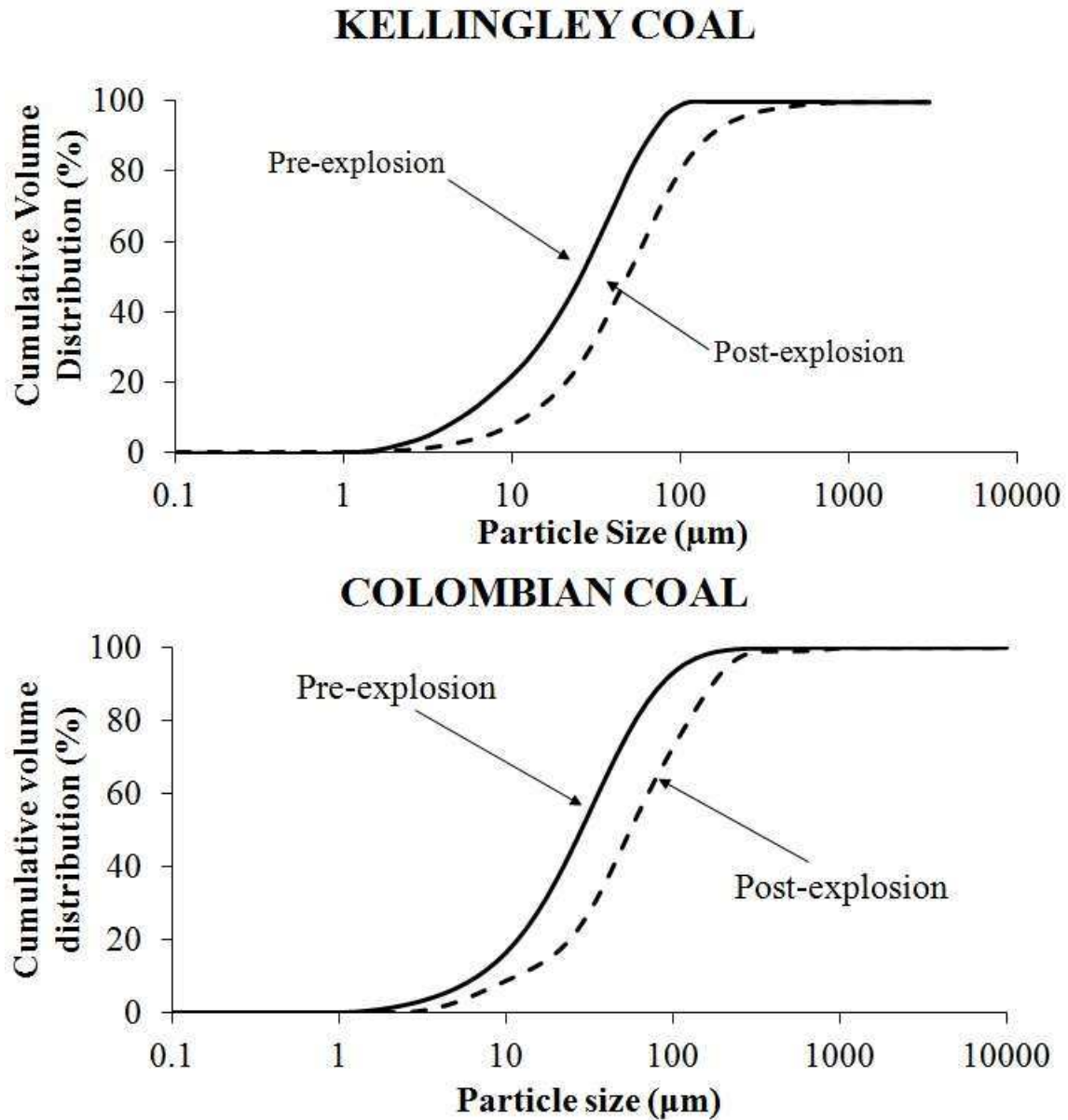


Figure 14. Particle size distribution of original and residual samples of Kellingley coal and Colombian coal

4. Conclusions

Despite having very similar composition Colombian coal and Kellingley coal presented very different reactivity: Colombian coal had higher K_{St} , flame speeds and heat release, MW/m^2 .

The main differences between the fuels were:

1. Surface area of Colombian coal particles was 4 times higher than for Kellingley coal
2. The rate at which the fixed carbon was burnt was faster for Colombian coal

The rate of reaction (and therefore K_{St}) appeared to be affected by the large surface area of Colombian coal particles. This could be due to the greater surface area for volatile release as well as more surface area for oxygen-carbon oxidation. This proves that particle structure can influence the rate of the combustion reaction and therefore the explosion reactivity of coal.

Residue analysis showed that for Kellingley coal, being less reactive, residues were closer to the original fuel composition than for Colombian coal. In explosion flame propagation the action of the expansion induced wind ahead of the flame is to entrain dust and impact it on the wall, where it does not take part in the explosion. About 50% of the initial mass injected did not participate in the explosion. The actual concentration of flame propagation is then NOT that of the injected concentration. This unburned mass was measured and enabled the actual equivalence ratio of the dust propagating flame front to be determined.

Explosion characteristics of both samples fell within the somewhat wide range of values available in the literature. Maximum pressures, MECs and flame speeds measured also reflected the difference in reactivity.

Two pulverised woody biomass were characterised and compared with the coal results. These had K_{St} and flame speeds close to that of Kellingley coal, in spite of differences in their composition, ash and particle size distributions. A literature search of other measurements of K_{St} and P_{max} showed that there was a wide range of reactivities in the literature for both biomass and coal. It is not generally true that biomass is more reactive than coal. Biomass can be more reactive than some coals and less reactive than other coals. The present results show that biomass and coal have a similar range of reactivities and peak pressures.

Acknowledgements

The authors are grateful to the Energy Program (Grant EP/H048839/1) for financial support. The Energy Program is a Research Councils UK cross council initiative led by EPSRC and contributed to by ESRC, NERC, BBSRC and STFC.

References

- [1] World Coal Association. Coal and electricity generation. 2012. In: <http://www.worldcoal.org/resources/coal-statistics/coal-matters/> World Coal Association.
- [2] DECC, Digest of UK energy statistics (DUKES), The Stationery Office, Norwich
- [3] Nalbandian, H. Performance and risks of advanced pulverised coal plants, *Energieia*, 2009; 20.
- [4] Eckhoff, RK. *Dust Explosions in the Process Industries*. 3rd ed. USA: Gulf Professional Publishing; 2003.
- [5] Palmer, KN. *Dust explosions and fire*. London: Chapman & Hall; 1973.
- [6] Nagy, J, Dorsett, HG, Cooper, AR. Explosibility of carbonaceous dusts, in: R.I. 6597, Washington, D.C., 1965, pp. p. 30.
- [7] Woskoboenko, F. Explosibility of Victorian brown coal dust, *Fuel*, 1988; 67: 1062-1068.
- [8] Amyotte, PR, Mintz, KJ, Pegg, MJ, Sun, Y-H, Wilkie, KI. Laboratory investigation of the dust explosibility characteristics of three Nova Scotia coals, *J. Loss. Prevent. Proc.*, 1991; 4: 102-109.
- [9] Continillo, G, Crescitelli, S, Furno, E, Napolitano, F, Russo, G. Coal dust explosions in a spherical bomb, *J. Loss. Prevent. Proc.*, 1991; 4: 223-229.
- [10] Wilén, C, Moilanen, A, Rautalin, A, Torrent, J, Conde, E, Lödel, R, Carlson, D, Timmers, P, Brehm, K. Safe handling of renewable fuels and fuel mixtures, in, VTT Technical Research Centre of Finland, Espoo, 1999, pp. 117 p.+app. 118p.

- [11] Cashdollar, KL. Coal dust explosibility, *J. Loss. Prevent. Proc.*, 1996; 9: 65-76.
- [12] Norman, F, Berghmans, J, Verplaetsen, F. The Dust Explosion Characteristics of Coal Dust in an Oxygen Enriched Atmosphere, *Procedia Engineering*, 2012; 45: 399-402.
- [13] Pilão, R, Ramalho, E, Pinho, C. Overall characterization of cork dust explosion, *J. Hazard. Mater.*, 2006; 133: 183-195.
- [14] Sattar, H, Phylaktou, HN, Andrews, GE, Gibbs, BM. Explosions and flame propagation in nut-shell biomass powders, in: IX International Symposium on Hazards, Prevention and Mitigation of Industrial Explosions, Cracow, Poland, 2012.
- [15] Callé, S, Klabá, L, Thomas, D, Perrin, L, Dufaud, O. Influence of the size distribution and concentration on wood dust explosion: Experiments and reaction modelling, *Powder Technol.*, 2005; 157: 144-148.
- [16] Garcia-Torrent, J, Conde-Lazaro, E, Wilen, C, Rautalin, A. Biomass dust explosibility at elevated initial pressures, *Fuel*, 1998; 77: 97.
- [17] Conde Lazaro, E, Garcia Torrent, J. Experimental research on explosibility at high initial pressure of combustible dusts, *J. Loss. Prevent. Proc.*, 2000; 13: 221-228.
- [18] Melin, S. Determination of explosibility of dust layers in pellet manufacturing plants, in: WPAC, Wood Pellet Association of Canada, 2012.
- [19] Bartknecht, W. *Dust Explosions: Course, prevention, protection*. London: Springer London; 1989.
- [20] Amyotte, PR, Cloney, CT, Kahn, FI, Ripley, RC. Dust explosion risk moderation for flocculent dusts, *J. Loss. Prevent. Proc.*, 2012; 25: 862-869.

- [21] Proust, C, Accorsi, A, Dupont, L. Measuring the violence of dust explosions with the “20l sphere” and with the standard “ISO 1m³ vessel” Systematic comparison and analysis of the discrepancies, *J. Loss. Prevent. Proc.*, 2007; 20: 599-606.
- [22] Wong, D, Huntley, S, Lehmann, BF, Zeeuwen, P. Sawmill wood dust sampling, analysis and explosibility. 2013. In: <https://fpinnovations.ca/Extranet/Pages/AssetDetails.aspx?item=/Extranet/Assets/ResearchReportsWP/3091.pdf#.VCUZ-fldVR0> FPIinnovations. Final report 301007168.
- [23] Krazinski, JL, Buckius, RO, Krier, H. Coal dust flames: A review and development of a model for flame propagation, *Prog. Energy Combust. Sci.*, 1979; 5: 31-71.
- [24] Smoot, LD, Pratt, DT. Pulverized coal combustion and gasification: Theory and applications for continuous flow processes. New York and London: Plenum Press; 1979.
- [25] Di Benedetto, A, Russo, P. Thermo-kinetic modelling of dust explosions, *J. Loss. Prevent. Proc.*, 2007; 20: 303-309.
- [26] Di Nola, G, de Jong, W, Spliethoff, H. The fate of main gaseous and nitrogen species during fast heating rate devolatilization of coal and secondary fuels using a heated wire mesh reactor, *Fuel Process. Technol.*, 2009; 90: 388-395.
- [27] Hertzberg, M, Zlochower, IA, Cashdollar, KL. Volatility model for coal dust flame propagation and extinguishment, *Symposium (International) on Combustion*, 1988; 21: 325-333.
- [28] Bradley, D, Dixon-Lewis, G, El-Din Habik, S. Lean flammability limits and laminar burning velocities of CH₄-air-graphite mixtures and fine coal dusts, *Combust. Flame*, 1989; 77: 41-50.
- [29] Sattar, H, Phylaktou, HN, Andrews, GE, Gibbs, BM. Pulverised biomass explosions: Investigation of the ultra rich mixtures that give peak reactivity, in: *IX International Symposium on Hazard, Prevention and Mitigation of Industrial Explosions*, Cracow, Poland, 2012.

[30] Jensen, B, Gillies, A. Review of coal dust explosibility research. In: Australasian Institute of Mining and Metallurgy, AusIMM, 9-14.

[31] International Organization of Standardization. 1928:2009. Solid mineral fuels. Determination of gross calorific value by the bomb calorimetric method and calculation of net calorific value. Geneva: ISO, 2009.

[32] Sattar, H, Huescar Medina, C, Phylaktou, HN, Andrews, GE, Gibbs, BM. Calibration of a 10L volume dust holding pot for the 1m³ standard vessel, for use in low bulk density biomass explosibility testing. In: 7th International Seminar on Fire and Explosion Hazards, May 5-10, Providence, USA. Singapore: Research publishing, 2013, 791-800.

[33] Slatter, DJF, Huescar Medina, C, Sattar, H, Andrews, G, Phylaktou, HN, Gibbs, BM. Biomass explosion residue analysis, in: X International Symposium on Hazards, Prevention and Mitigation of Industrial Explosions, Bergen, Norway, 2014.

[34] Sattar, H, Andrews, G, Phylaktou, HN, Gibbs, BM. Turbulent flame speeds and laminar burning velocities of dusts using the ISO 1m³ dust explosion method, Chem. Eng. Trans., 2014; 36: 157-162.

[35] Harris, RJ. The investigation and control of gas explosions and heating plant. London: E&FN Spon in association with the British Gas Corporation; 1983.

[36] Ng, DL, Cashdollar, KL, Hertzberg, M, Lazzara, CP. Electron Microscopy Studies of Explosion and Fires Residues, in: IC 8936, Dept. of the Interior, Bureau of Mines, Washington D.C, 1983.

[37] Cashdollar, KL. Overview of Dust Explosibility Characteristics, J. Loss. Prevent. Proc., 2000; 13: 183-199.

[38] Slatter, DJF, Huescar Medina, C, Sattar, H, Andrews, GE, Phylaktou, HN, Gibbs, BM. The influence of particle size and volatile content on the reactivity of CH and CHO chemical and biomass

dusts. In: 7th International Seminar on Fire and Explosion Hazards, 5-10 May, Providence, USA. Singapore: Research Publishing, 2013, 109.

[39] Basu, P. Combustion and gasification in fluidised beds. Boca Raton, FL: CRC Press Taylor & Francis Group; 2006.

[40] Kuprianov, VI, Tanetsakunvatana, V. Assessment of gaseous, PM and trace element emissions from a 300-MW lignite-fired boiler unit for various fuel qualities, Fuel, 2006; 85: 2171-2179.

[41] Huescar Medina, C, Sattar, H, Phylaktou, HN, Andrews, GE, Gibbs, BM. Explosion reactivity characterisation of pulverised torrefied spruce wood, in: X International Symposium on Hazards, Protection and Mitigation of Industrial Explosions, Bergen, Norway, 2014.